

Transepithelial transport of P-glycoprotein substrate by the malpighian tubules of the desert locust

Article (Published Version)

Rossi, Marta, De Battasti, Davide De and Niven, Jeremy Edward (2019) Transepithelial transport of P-glycoprotein substrate by the malpighian tubules of the desert locust. PLoS ONE, 14 (10). pp. 1-23. ISSN 1932-6203

This version is available from Sussex Research Online: <http://sro.sussex.ac.uk/id/eprint/89908/>

This document is made available in accordance with publisher policies and may differ from the published version or from the version of record. If you wish to cite this item you are advised to consult the publisher's version. Please see the URL above for details on accessing the published version.

Copyright and reuse:

Sussex Research Online is a digital repository of the research output of the University.

Copyright and all moral rights to the version of the paper presented here belong to the individual author(s) and/or other copyright owners. To the extent reasonable and practicable, the material made available in SRO has been checked for eligibility before being made available.

Copies of full text items generally can be reproduced, displayed or performed and given to third parties in any format or medium for personal research or study, educational, or not-for-profit purposes without prior permission or charge, provided that the authors, title and full bibliographic details are credited, a hyperlink and/or URL is given for the original metadata page and the content is not changed in any way.

RESEARCH ARTICLE

Transepithelial transport of P-glycoprotein substrate by the Malpighian tubules of the desert locust

Marta Rossi^{1*}, Davide De Battisti², Jeremy Edward Niven^{1,3*}

1 School of Life Sciences, University of Sussex, Falmer, Brighton, United Kingdom, **2** Department of Bioscience, Swansea University, Swansea, Singleton park, Wales, United Kingdom, **3** Centre for Computational Neuroscience and Robotics, University of Sussex, Falmer, Brighton, United Kingdom

* M.Rossi@sussex.ac.uk (MR); J.E.Niven@sussex.ac.uk (JEN)



OPEN ACCESS

Citation: Rossi M, De Battisti D, Niven JE (2019) Transepithelial transport of P-glycoprotein substrate by the Malpighian tubules of the desert locust. PLoS ONE 14(10): e0223569. <https://doi.org/10.1371/journal.pone.0223569>

Editor: Subba Reddy Palli, University of Kentucky, UNITED STATES

Received: July 20, 2019

Accepted: September 24, 2019

Published: October 8, 2019

Copyright: © 2019 Rossi et al. This is an open access article distributed under the terms of the [Creative Commons Attribution License](https://creativecommons.org/licenses/by/4.0/), which permits unrestricted use, distribution, and reproduction in any medium, provided the original author and source are credited.

Data Availability Statement: All relevant data are within the manuscript and its Supporting Information files.

Funding: M.R. was financially supported by a graduate studentship from the School of Life Sciences, University of Sussex. D.D.B. was financially supported by the Welsh government/ HEFCW RESILCOAST project. The funders had no role in study design, data collection and analysis, decision to publish, or preparation of the manuscript.

Abstract

Extrusion of xenobiotics is essential for allowing animals to remove toxic substances present in their diet or generated as a byproduct of their metabolism. By transporting a wide range of potentially noxious substrates, active transporters of the ABC transporter family play an important role in xenobiotic extrusion. One such class of transporters are the multi-drug resistance P-glycoprotein transporters. Here, we investigated P-glycoprotein transport in the Malpighian tubules of the desert locust (*Schistocerca gregaria*), a species whose diet includes plants that contain toxic secondary metabolites. To this end, we studied transporter physiology using a modified Ramsay assay in which *ex vivo* Malpighian tubules are incubated in different solutions containing the P-glycoprotein substrate dye rhodamine B in combination with different concentrations of the P-glycoprotein inhibitor verapamil. To determine the quantity of the P-glycoprotein substrate extruded we developed a simple and cheap method as an alternative to liquid chromatography–mass spectrometry, radiolabelled alkaloids or confocal microscopy. Our evidence shows that: (i) the Malpighian tubules contain a P-glycoprotein; (ii) tubule surface area is positively correlated with the tubule fluid secretion rate; and (iii) as the fluid secretion rate increases so too does the net extrusion of rhodamine B. We were able to quantify precisely the relationships between the fluid secretion, surface area, and net extrusion. We interpret these results in the context of the life history and foraging ecology of desert locusts. We argue that P-glycoproteins contribute to the removal of xenobiotic substances from the haemolymph, thereby enabling gregarious desert locusts to maintain toxicity through the ingestion of toxic plants without suffering the deleterious effects themselves.

Introduction

Insect excretory systems consist primarily of the Malpighian tubules and the hindgut, which act synergistically to regulate haemolymph composition [1,2]. Malpighian tubules are blind ended tubules that float in the haemolymph and empty into the gut at the midgut-hindgut

Competing interests: The authors have declared that no competing interests exist.

junction, secreting primary urine, the composition of which is modified by water and ion reabsorption in the hindgut [3]. The tubules are considered analogous to vertebrate nephrons [2]. Cells of the epithelium forming the tubule wall express primary and secondary active transporters that move K^+ , Na^+ and Cl^- ions into the lumen creating an osmotic gradient that produces water secretion (for a review see [4]). Insects regulate ion and water secretion according to their feeding habits and ecological niche. For example, haematophagous insects must cope with an excess of NaCl and water after a blood meal [5], whereas phytophagous insects must often cope with a diet rich in K^+ as well as with secondary metabolites [6,7].

In addition to osmoregulation, Malpighian tubules play a fundamental role in the removal of metabolic waste and potentially noxious substances that have been ingested [1,8]. Alkaloids and organic anions and cations are actively transported by ATP-dependant transporters such as the multidrug resistance-associated protein 2 (MRP2) and P-glycoproteins (P-gps, multidrug resistance protein (MDR1) or ABCB1), both members of the ABC transporter family [9,10]. Multidrug resistance-associated protein 2 (MRP2) transporters are involved in the transport of organic anions [11,12], while P-glycoproteins transport type II organic cations (>500 Da), hydrophobic and often polyvalent compounds (e.g. alkaloids and quinones) [13].

The presence and physiology of these multidrug transporters have been explored using specific substrates and selective inhibitors (e.g. [9,11,14]). In the Malpighian tubules of the cricket (*Teleogryllus commodus*) and the fruit fly (*Drosophila melanogaster*), the transepithelial transport of the fluorescent MRP2 substrate Texas Red is reduced by the MRP2 inhibitors MK571 and probenecid [11], while the transport of the fluorescent P-glycoprotein substrate daunorubicin is selectively reduced by the P-glycoprotein inhibitor verapamil [11]. The transport of nicotine by P-glycoprotein transporters has also been demonstrated in numerous insect species, including the tobacco hornworm (*Manduca sexta* [9]), fruit fly (*D. melanogaster*), kissing bug (*Rhodnius prolixus*), large milkweed bug (*Oncopeltus fasciatus*), yellow fever mosquito (*Aedes aegypti*), house cricket (*Acheta domesticus*), migratory locust (*Locusta migratoria*), mealworm beetle (*Tenebrio molitor*), American cockroach (*Periplaneta americana*) and cabbage looper (*Trichoplusia ni*) [15]. In insects, the understanding of the interaction between xenobiotics (i.e. insecticides, herbicides, miticides and secondary plant metabolites) and P-glycoprotein transporters is still limited, but there is an increasing interest in understanding how different xenobiotics can act synergistically to maximize the efficacy of insecticides in pests or impair the xenobiotic detoxification of beneficial insects such as honey bees [16].

Desert locusts (*Schistocerca gregaria*) are generalist phytophagous insects with aposematic coloration in the gregarious phase. They feed on a wide range of plants including those, such as *Schouwia purpurea* and *Hyoscyamus muticus*, that contain toxins to become unpalatable and toxic to predators [17–20]. Nevertheless, it is likely that gregarious desert locusts excrete some of the toxins that they ingest, relying instead on their gut contents to maintain toxicity [21,22]. Two lines of evidence suggest that this excretion is likely to involve P-glycoproteins: (1) they are expressed in the Malpighian tubules of numerous species (e.g. *A. domesticus*, *L. migratoria*, *P. americana*) from orthopteroid orders [15]; and (2) they are expressed in the blood brain barrier of the desert locust [23]. However, P-glycoproteins in the Malpighian tubules of desert locusts have not been studied previously.

Here we show that xenobiotic transport and extrusion in the Malpighian tubules of the desert locust is an active process dependent upon P-glycoprotein like transporters using isolated tubules to perform a modified Ramsay secretion assay [24]. We evaluated the extrusion of the P-glycoprotein substrate dye rhodamine B (e.g. [25,26]) with or without the addition of the selective P-glycoprotein inhibitor verapamil (e.g. [23,27,28]). Our results suggest that P-glycoprotein transporters may play an important role in the xenobiotic extrusion in the Malpighian tubules of the desert locust. By using linear mixed effect models to account for repeated

observations of single tubules and obtaining multiple tubules from single locusts, we found that tubule surface area more accurately predicts fluid secretion rate than diameter or length. Moreover, this statistical model allowed us to quantify the influence of the surface area on the fluid secretion rate in different treatments, and how it changes over time. We found that the surface area of the tubules positively influences their fluid secretion rate and that the fluid secretion rate influences the net extrusion of rhodamine B. We propose that this assay may be used in future to understand the physiology of the P-glycoproteins when exposed to a wide range of different substances.

Materials and methods

Animals

Fifth instar desert locusts (*Schistocerca gregaria*; Forskål, 1775) were obtained from Peregrine Livefoods (Essex, UK) and raised under crowded conditions at 28–30°C with 12:12 photoperiod. Locusts were fed with organic lettuce, fresh wheat seedlings and wheat germ *ad libitum*. Fifth instar nymphs were checked daily and, within 24 hours post-eclosion, were marked with acrylic paint (Quay Imports Ltd, Kirkham, Lancashire, UK). Only adult males between 20 and 22 days post-eclosion were used in the experiments.

Saline and chemicals

The saline used was adapted from the Ringer solution of Maddrell and Klunswan [6]. Its composition was: 5.73 g/L NaCl (98 mM), 0.30 g/L KCl (4 mM), 2 mL CaCl₂ solution 1M (2 mM), 1.86 g/L NaHCO₃ (22 mM), 1.09 g/L NaH₂P0₄·2H₂O (7 mM), 0.19 g/L MgCl₂ (2 mM), 1.80 g/L glucose (10 mM), 0.83 g/L sodium glutamate (4.9 mM), 0.88 g/L sodium citrate (3.5 mM) and 0.37 g/L malic acid (2.8 mM). The final pH of the saline was 7.15. It was stored at 4°C for a maximum of three days. Stock solutions of rhodamine B (50 mM and 3 mM) and verapamil hydrochloride (20 mM) were prepared in water and diluted to the final concentration in the saline. Rhodamine B was applied at 60 µM and verapamil at 125 µM or 250 µM. All chemicals were purchased from Sigma-Aldrich (UK) or Fisher Scientific (UK).

Locust dissection

The locusts were placed in the freezer for 4–5 minutes until sedated. Upon removal from the freezer, the abdomen was cut transversely ~5 mm from the anus, and holding the head with one hand and the thorax with the other hand, the head was pulled away from the remainder of the body (Fig 1A) [6]. In this way, the entire gut with the Malpighian tubules attached was removed from the body. The gut was placed onto an 8 cm Sylgard[®] 184 (Dow Corning, Midland, MI, USA) coated Petri dish, filled with saline. The head was separated from the saline using modelling clay (Plasticine[®]) (Fig 1B). The preparation was pinned at the cut distal end of the gut to prevent it from floating.

Malpighian tubules dissection

Using a Nikon SMZ-U (Nikon Corp., Tokyo, Japan) stereoscopic microscope, the Malpighian tubules were removed by gently pulling the distal part to release them from the gut and cutting the proximal end at ~5 mm from the gut). Each isolated tubule was moved immediately into a 30 µL drop of saline on a 5 cm Sylgard[®] coated Petri dish and covered with paraffin oil to prevent desiccation. Both ends of each Malpighian tubule were pulled out from the saline drop in opposite directions and wrapped around steel pins pushed into the Sylgard[®] layer (Fig 1C and 1D). Three anterior tubules were removed from each locust. Tracheae coiled around the distal

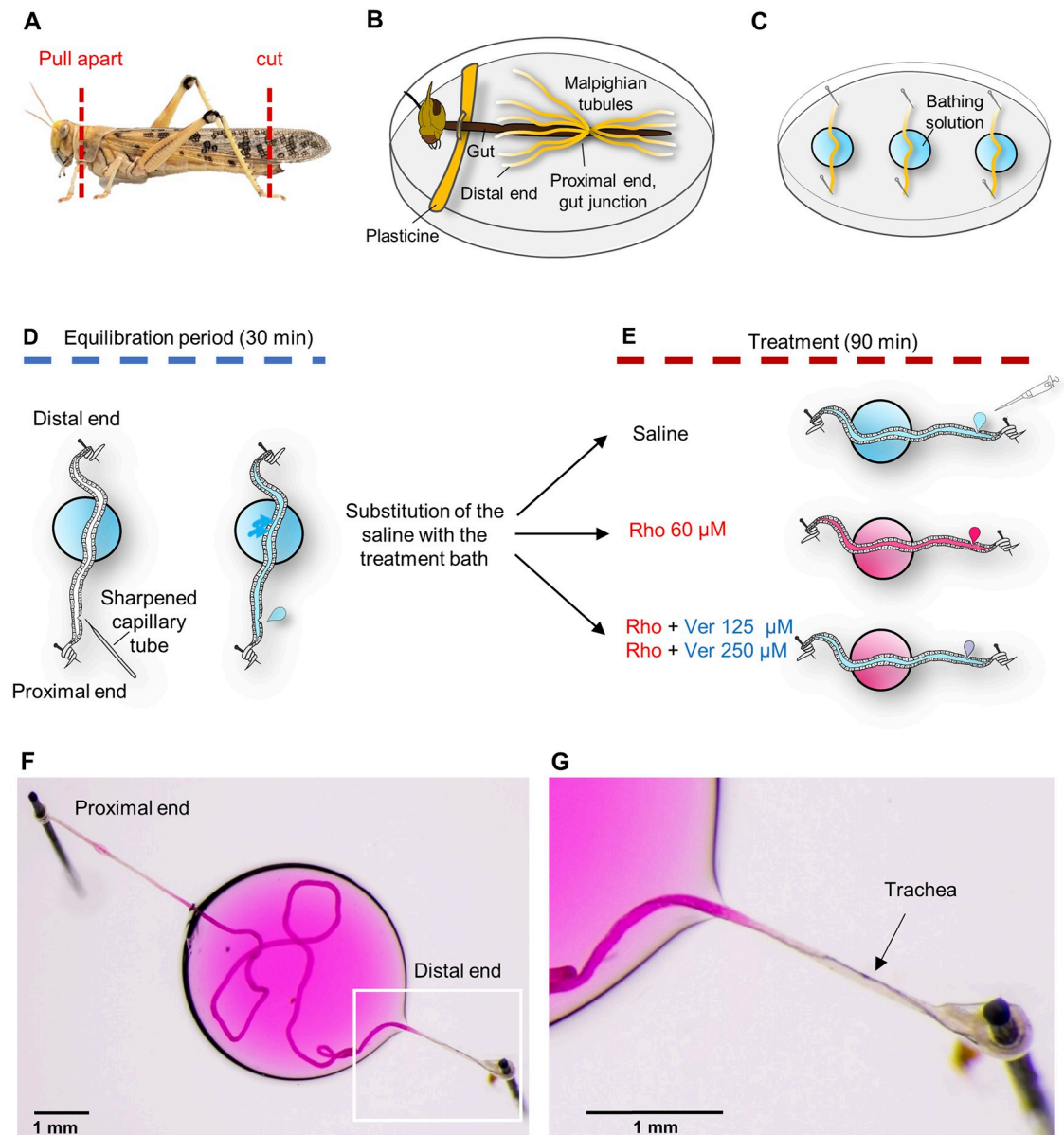


Fig 1. Preparation of Malpighian tubules for *ex vivo* experimentation from the desert locust, *Schistocerca gregaria*, and experimental scheme for assaying the presence of P-glycoproteins within the Malpighian tubules. (A) Cutting the posterior tip of the abdomen permits removal of the head and the fully intact gut. (B) The gut is submerged in saline and the Malpighian tubules are exposed. The head is separated from the saline bath by a barrier of modelling clay. (C) Three tubules are removed from each locust and fixed on a Sylgard[®] surface traversing a small drop of bathing solution, and covered with paraffin oil. (D) The proximal and distal ends of individual tubules are wound around Minuten pins to fix them. Once the saline bath and paraffin oil have been applied, the proximal end of the tubule is punctured with a sharpened capillary tube to allow fluid secretion. After 30 minutes of equilibration the saline bath was replaced by a bath containing one of the treatments. (E) Every 30 minutes the secreted droplet was removed, placed on the Petri dish and photographed. (F) An Example of an isolated Malpighian tubule to perform a modified Ramsay secretion assay. The middle section of the tubule is immersed in the bathing solution with the respective treatment, while the proximal and distal ends are fixed outside. (G) Detail of the distal end with the trachea visible. Only a small part of the trachea is immersed in the bath.

<https://doi.org/10.1371/journal.pone.0223569.g001>

part of the tubule were not removed to prevent any damage of the tubule surface (Fig 1F and 1G).

Fluid secretion (Ramsay) assay

Using a sharpened glass capillary tube, each tubule was punctured near the proximal end to allow the fluid secretion (Fig 1D). The tubule was allowed to equilibrate for 30 minutes at which point the saline bath was replaced with 30 μ L drop containing one of the four different treatments we tested: (i) saline, (ii) rhodamine B 60 μ M, (iii) rhodamine B 60 μ M + verapamil 125 μ M, (iv) rhodamine B 60 μ M + verapamil 250 μ M (Fig 1E). The first droplet secreted after the bath replacement was discarded. For the subsequent 90 minutes, the secreted droplet was removed at intervals of 30 minutes (Fig 1E and 1F) using a P10 pipette (Gilson Scientific UK, Dunstable, Bedfordshire, UK) and photographed with a digital camera (Canon EOS 7D; Canon, Tokyo, Japan) mounted with two custom attachments (Best scientific A clamp via 1.6 x Canon mount; Leica 10445930 1.0 x) on the stereoscopic microscope (Nikon SMZ-U; Nikon Corp., Tokyo, Japan). Images were shot in raw format and processed with ImageJ v.1.51p software [29]. To prevent the photobleaching of the rhodamine B, we minimised light exposure by conducting the experiment under red light and keeping the sample in a custom designed dark box between measurements.

Droplet measurement

The diameter (μ m) of each secreted droplet (S1 Fig) was measured to calculate its volume (nL) using the sphere formula, where V is the drop volume and d the droplet diameter. The volume was converted from μ m³ to nL using the formula:

$$V = \frac{4}{3} \pi \left(\frac{d}{2} \right)^3 10^{-6}.$$

For each tubule, we calculated the fluid secretion rate (nL/min), given by the droplet volume divided by the time between samples (30 mins). For each droplet, we also measured colour intensity to estimate the rhodamine B concentration (μ M) from a calibration curve (see below). To estimate the number of moles of rhodamine B extruded per minute, we calculated the net extrusion of rhodamine B (fmol/min) as the product of the fluid secretion rate and the rhodamine B concentration.

Rhodamine B calibration curve

The intensity of the droplets depends not only on rhodamine B concentration, but also on the droplet diameter (S2 and S3 Figs). So, we constructed a calibration curve for rhodamine B concentration to estimate the rhodamine B concentration of the droplets secreted. We prepared standard solutions of known rhodamine B concentrations: 0, 15, 30, 50, 60, 75, 120, 150, 240 and 480 μ M. For each concentration, droplets of different sizes were placed on a Petri dish coated with Sylgard[®] and covered with paraffin oil. We photographed the droplets against a white background at the same light intensity, and white balancing the camera before shooting. All the images were analysed subsequently using ImageJ v.1.51p software [29].

Droplet colour varied from white (transparent droplet at rhodamine B concentration = 0 μ M) to intense pink, depending upon the rhodamine B concentration. We split each image into the component colour channels and measured the intensity of the green channel. To control for the background, we compared the mean intensity inside the droplet with that outside using the formula $I = I_i - I_o$, where I is the intensity, I_i is the intensity inside the droplet, and

I_o is the intensity outside the droplet. We used a range of droplet diameters from 138 μm to 999 μm .

To validate the reliability of using the green channel, we also measured the magenta channel and the total intensity using Adobe Photoshop CC v. 19.1.1 (Adobe Systems Incorporated, CA, USA). Both the magenta channel and total intensity correlated with the intensity of green channel (Pearson's correlation, Magenta: $p < 0.001$, $df = 17$, $R^2 = 1$; Total intensity: $p < 0.001$, $df = 17$, $R^2 = 0.99$).

The relationship between the intensity and the rhodamine concentration depends upon the diameter of the droplet (S2 Fig). For each droplet diameter rank, the relationship between the intensity measured and the known rhodamine concentration can be described by a linear model. To determine the rhodamine concentration given the intensity and the diameter of the droplets, for each diameter rank we ran a linear regression model forced through the origin, with intensity as the independent variable and rhodamine concentration as the response variable (linear model: rhodamine concentration \sim intensity-1). Hence, for each diameter rank we obtained the equation that predicts the rhodamine concentration from the intensity measured, given a specific diameter (S2 Fig).

The slope of the linear equations decreases as the diameter increases, following an exponential decay (S3A Fig). To obtain the equation that predicts the slope of the linear equations for a given diameter, we log transformed both axis and we ran a log-level regression model (Linear model: $\log(\text{slope}) \sim \log(\text{droplet diameter})$; S3B Fig). The resulting equation was:

$$\log(\text{slope})_i = -1.44 \cdot \log(\text{diameter})_i + 10.38.$$

Using the predict command in R, we used the model to predict the slope value (back transformed to the original scale) for each diameter of the droplets we collected in the experiment. Finally, we multiplied the slope value for the intensity measured to calculate the rhodamine concentration of each droplet.

Malpighian tubule measurement

At the end of the assay, the tubule was photographed to measure its diameter (μm). The length (mm) of the tubule in contact with the treatment solution, was measured by cutting off the two extremities of the tubule outside the bath, laying the remaining section of tubule flat on the Sylgard[®] base, and photographing it. The surface (mm^2) of the tubule in contact with the bath, was calculated from the cylinder formula: $S = 2\pi \left(\frac{d}{2}\right) l$, where S is the tubule surface, d is the tubule diameter, and l is the tubule length.

Statistical analysis

All the statistical analysis was conducted in R version 3.4.1 [30]. We performed Linear Mixed Effect Models (LMEM) by restricted maximum likelihood (REML) estimation by using the lmer function from the 'lme4' package [31]. We used the Akaike information criterion (AIC) [32] for model selection. Significances of the fixed effects were determined using Satterthwaite's method for estimation of degrees of freedom by using the anova function from the 'lmerTest' [33]. The non-significant interactions ($P > 0.05$) were removed. However, we retained all the main effects even if they were not statistically significant to avoid an increase in the type I error rate [34]. Estimated marginal means and pairwise comparisons were obtained using the 'lsmeans' package [35] and the p value adjusted with the Tukey method. All plots were made using the 'ggplot2' package [36].

To investigate the effect of the treatments on the fluid secretion rate and the net extrusion of rhodamine B, we analysed the interaction between the treatment (categorical), time of

incubation (categorical) and the surface area (continuous (mm^2)). For the rhodamine B concentration, we analysed the interaction between treatment (categorical) and time (categorical). To account for the nested structure of data, we included the individual locust as random intercept in the model. We also included tubule identity as a random intercept and time as random slope to account for the repeated measurements on the same individual tubule. To investigate the effect of the fluid secretion rate on the net extrusion of rhodamine B we analysed the interaction of the variables secretion rate, treatment and time including as before the individual locust as random intercept, and tubule identity as a random intercept and time as random slope. To simplify the interpretation of the regression estimates, we centred the surface variable on its mean. Therefore, all the estimates and comparisons are referred to a tubule with a mean surface area.

All relevant data underlying the findings of our study are included in the supplementary information: [S1](#), [S2](#) and [S3](#) Files.

Results

We prepared three Malpighian tubules from each locust (see [Materials and methods](#); [Fig 1](#)). Each tubule was punctured near the proximal end to allow the luminal fluid to be secreted and then they were allowed to equilibrate in the saline bath for 30 minutes ([Fig 1D](#)). The saline bath was then replaced with one of four treatments: saline (control); rhodamine B 60 μM (R60); rhodamine B 60 μM + verapamil 125 μM (V125); and rhodamine B 60 μM + verapamil 250 μM (V250) ([Fig 1E](#)). Six locusts were used for each of the treatments except for the R60 treatment in which eight locusts were used. Every 30 minutes the droplet secreted by the tubule during the Ramsay assay was removed.

Fluid secretion rate and surface area

We determined the fluid secretion rate of each tubule from the volume of the droplet secreted after each 30-minute interval up to 90 minutes after the start of the treatment. Thus, for each tubule we had three measurements of the secretion rate in each of the four treatments. In total, there were 233 treatment observations (one droplet was lost after 60 minutes for the V250 treatment) from 78 Malpighian tubules.

To determine whether the surface area of the Malpighian tubules exposed to the bath solution influences the fluid secretion rate, we measured the length and diameter of each tubule immersed in the saline or treatment. By comparing linear mixed effect models that incorporated these measurements of length, diameter or surface area, we determined that surface area was the best explanatory variable ([S1 Table](#)). There was no difference in the surface area of Malpighian tubules exposed to the bathing solution among the treatments ($F_{3,22.02} = 0.488$, $p = 0.694$; Control: $2.00 \pm 0.09 \text{ mm}^2$ (mean \pm S.E.); R60: $2.01 \pm 0.06 \text{ mm}^2$; V125: $2.27 \pm 0.06 \text{ mm}^2$; V250: $2.29 \pm 0.07 \text{ mm}^2$).

The surface area of the tubule exposed in the bathing solution influenced the fluid secretion rate depending on the treatment ($F_{3,66.29} = 3.25$, $p = 0.027$; [Fig 2](#); [Table 1A](#)). Throughout the whole period of incubation, the surface area positively influenced the fluid secretion of tubules incubated in R60, V125 and Saline, while the V250 treatment the tubules showed no significant correlation between surface area and fluid secretion rate ([Fig 2C](#); [Table 1A](#)). Having incorporated tubule surface area into our statistical model, we were able to compare the fluid secretion rates of our control and treatments objectively. The fluid secretion rate decreased over time irrespective of the treatment ($F_{2,82.36} = 46.12$, $p < .001$; Time 60 vs Time 30: $-0.12 \pm 0.01 \text{ nL/min}$, $p < .001$; Time 90 vs Time 60: $-0.04 \pm 0.01 \text{ nL/min}$, $p = 0.013$; [Fig 3](#), [Table 1B](#)) and at each time point there was no significant difference between treatments ([Fig 3](#), [Table 1C](#)).

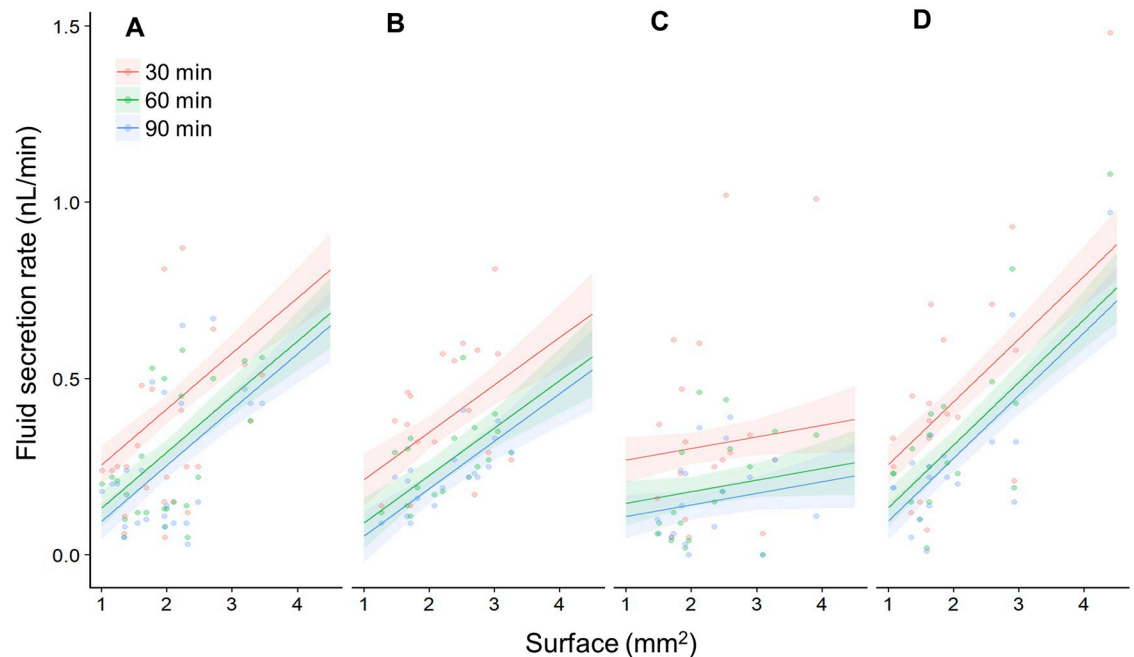


Fig 2. Tubule surface area positively influences the fluid secretion rate. (A) A plot of the surface area of the tubule exposed to the bath versus the fluid secretion rate for the R60 treatment every 30 minutes. (B) As in 'A' but for the V125 treatment. (C) As in 'A' but for V250 treatment. (D) As in 'A' but for the saline treatment. Small circles indicate the fluid secretion rates of individual tubules at a particular time point. Each line with the shaded area around represents the mixed effect model fit with the standard error.

<https://doi.org/10.1371/journal.pone.0223569.g002>

Renewing bath saline increases the fluid secretion rate

To exclude the possibility that the decrease in the fluid secretion rate was caused by a damage of the tubules during the Ramsay assay, we replaced the saline bath after 90 minutes with fresh saline, to determine whether tubules would increase their fluid secretion rate to previous levels. We removed three tubules from six locusts (17 tubules in total, one tubule excluded) and incubated them in saline for 90 minutes, removing the droplet secreted every 30 minutes. After 90 minutes the saline bath was removed, replaced with fresh saline. The tubules were then incubated for further 90 minutes removing the droplet secreted every 30 minutes. The secretion rate decreased after 60 and 90 minutes (S4 Fig, S2 Table), but increased after 120 minutes following replacement of the saline (S4 Fig, S2 Table).

Malpighian tubule integrity during the Ramsay assay

To exclude the possibility that manipulation during the Ramsay assay altered the diameter of the tubules, we measured the diameter of the tubules *in vivo*, at the beginning, and at the end of the assay. We found that the diameter of the tubules was unaffected by the assay and was comparable to the tubule's diameter *in vivo* (S5 Fig, S3A and S3B Table).

Net extrusion of Rhodamine B

We determined the concentration of Rhodamine B in each of the droplets collected from the Malpighian tubules exposed to the R60, V125 and V250 treatments at each time point. There was a significant interaction between treatment and time ($F_{4,73.19} = 15.19$, $p < .001$, Fig 4A), indicating that the rhodamine B concentration changed over time depending on the treatment (Table 2). The concentration of rhodamine B in the droplets significantly increased during the

Table 1. Outcomes of the linear mixed effect model investigating the effect of time of incubation, treatment, and surface area on the fluid secretion rate (SR) (nL/min) of Malpighian tubules.

A.	Treatment	Time 30, 60, 90 min		
		surface trend \pm se	P-value	
	R60	0.16 ± 0.04	< .001	
	V125	0.14 ± 0.05	0.006	
	V250	0.02 ± 0.04	0.569	
	Saline	0.16 ± 0.04	< .001	

B.	Treatment	Time 30 min	Time 60 min	Time 90 min	SR decrease between 30 and 60 min	SR decrease between 60 and 90 min
		Mean \pm se	Mean \pm se	Mean \pm se		
	R60	0.44 ± 0.05	0.32 ± 0.05	0.28 ± 0.04	-27%	-13%
	Saline	0.46 ± 0.05	0.33 ± 0.05	0.30 ± 0.05	-28%	-9%
	V125	0.36 ± 0.05	0.24 ± 0.05	0.20 ± 0.05	-33%	-17%
	V250	0.30 ± 0.05	0.18 ± 0.05	0.15 ± 0.05	-40%	-17%

C.	Treatment	Time 30, 60, 90 min		
		estimate \pm se	P-value	
	V125 vs R60	-0.08 ± 0.07	0.662	
	V250 vs R60	-0.13 ± 0.07	0.213	
	Saline vs R60	0.02 ± 0.07	0.995	
	V250 vs V125	-0.06 ± 0.07	0.850	
	Saline vs V125	0.09 ± 0.07	0.572	
	Saline vs V250	0.15 ± 0.09	0.182	

The model applied was (Secretion rate \sim surface * treatment + time + (1|locust) + (1+time|tubule)). (A) Estimates of the influence of each unit of surface (mm²) on the fluid secretion rate for each treatment. (B) Summary of the mean values for each treatment at each time point. (C) Pairwise comparisons between treatments for each time of incubation.

<https://doi.org/10.1371/journal.pone.0223569.t001>

incubation time in all the treatments (Table 1B, Fig 4A). In particular, the increase in rhodamine B concentration in the R60 treatment was more pronounced than in either the V125 or V250 treatments (Table 1C, Fig 4A). At each time point, the treatment significantly affected the rhodamine B concentration. Compared to the R60 treatment, the addition of verapamil in the V125 and V250 treatments reduced the rhodamine B concentration of the secreted droplets after 30, 60, and 90 minutes (Table 2D, Fig 4A). However, there was no significant difference in the rhodamine B concentration between the V125 and V250 treatments at any time point (Table 2D, Fig 4A).

We calculated the total number of moles of rhodamine B extruded by the Malpighian tubules per minute as the product of the secretion rate and the rhodamine B concentration of the droplets secreted, which we termed the net extrusion rate. There was an interaction between treatment, time and surface ($F_{4,74.59} = 2.56$, $p = 0.046$; Table 3, Figs 4B and 5A–5C), indicating that the dependency of the net extrusion of rhodamine B upon tubule surface area was influenced by the incubation time and the treatment (Table 3A and 3E, Fig 5A–5C). The net extrusion increased significantly between 30 and 60 minutes in all the treatments (Table 3B, Fig 4B). In contrast, between 60 and 90 minutes the net extrusion increased only for the tubules incubated in R60 and V250, whereas it remained steady for V125 treatments (Table 3B, Fig 4B). In particular, the net extrusion was more pronounced in the R60 treatment compared to V125 and V250 (Table 3C, Fig 4B). At each time point, the treatment affected the

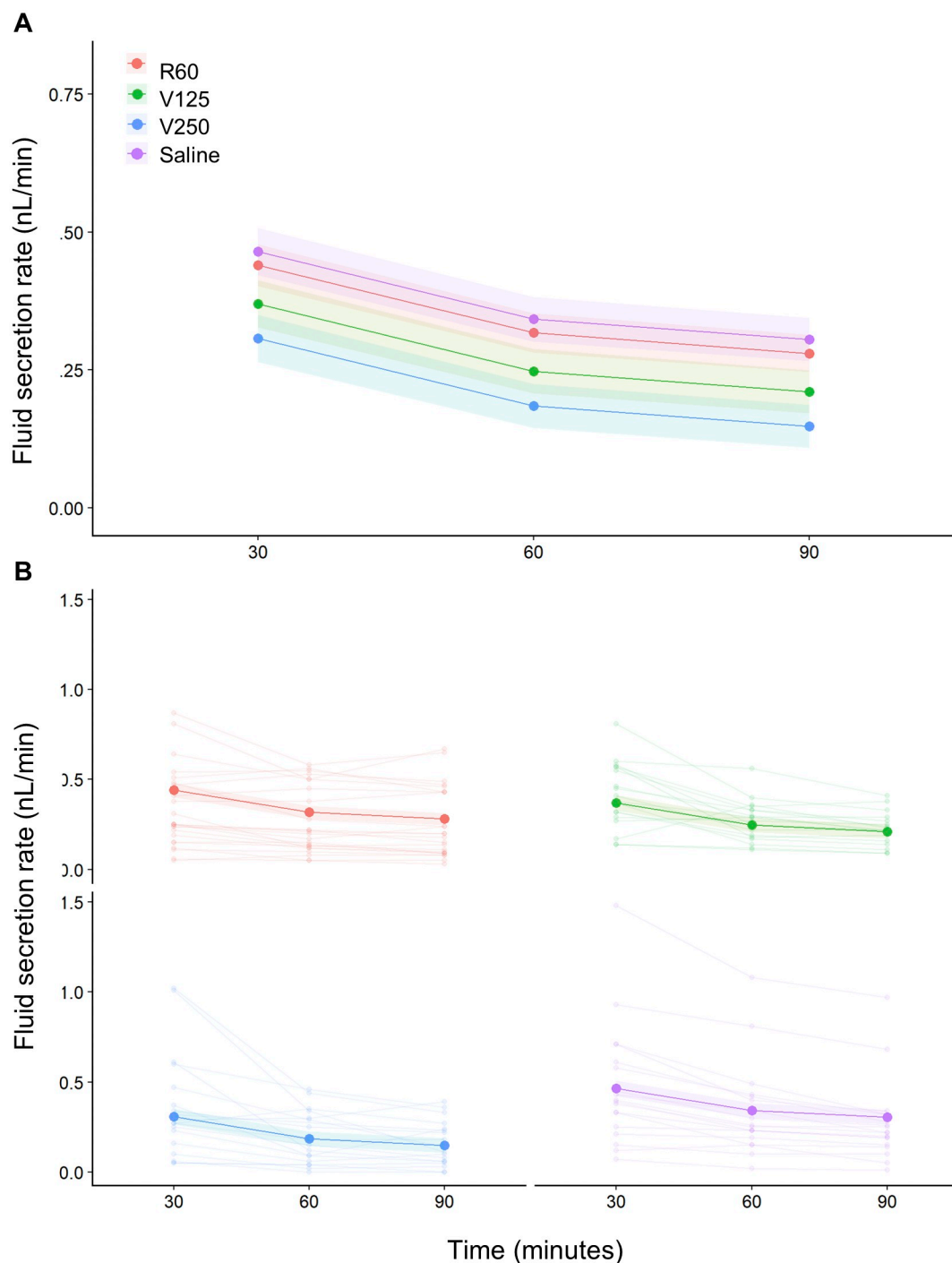


Fig 3. Mean fluid secretion rate of Malpighian tubules during the incubation period. (A) The mean fluid secretion rate decreased after 60 minutes of incubation in all the treatments, while it remained steady for the next 30 minutes in all the treatments except in the saline one. Each line with the shaded area around represents the mixed effect model fit with the standard error. (B) As in 'A', but with the fluid secretion rate of individual tubules shown by pale lines linking smaller dots.

<https://doi.org/10.1371/journal.pone.0223569.g003>

net extrusion of rhodamine B (Table 3D, Fig 4B). In comparison to the R60 treatment, the addition of verapamil in the V125 and V250 treatments significantly reduced the net extrusion of rhodamine B after 30, 60 and 90 minutes, however, there was no significant difference between the V125 and V250 treatments (Table 3D, Fig 4B).

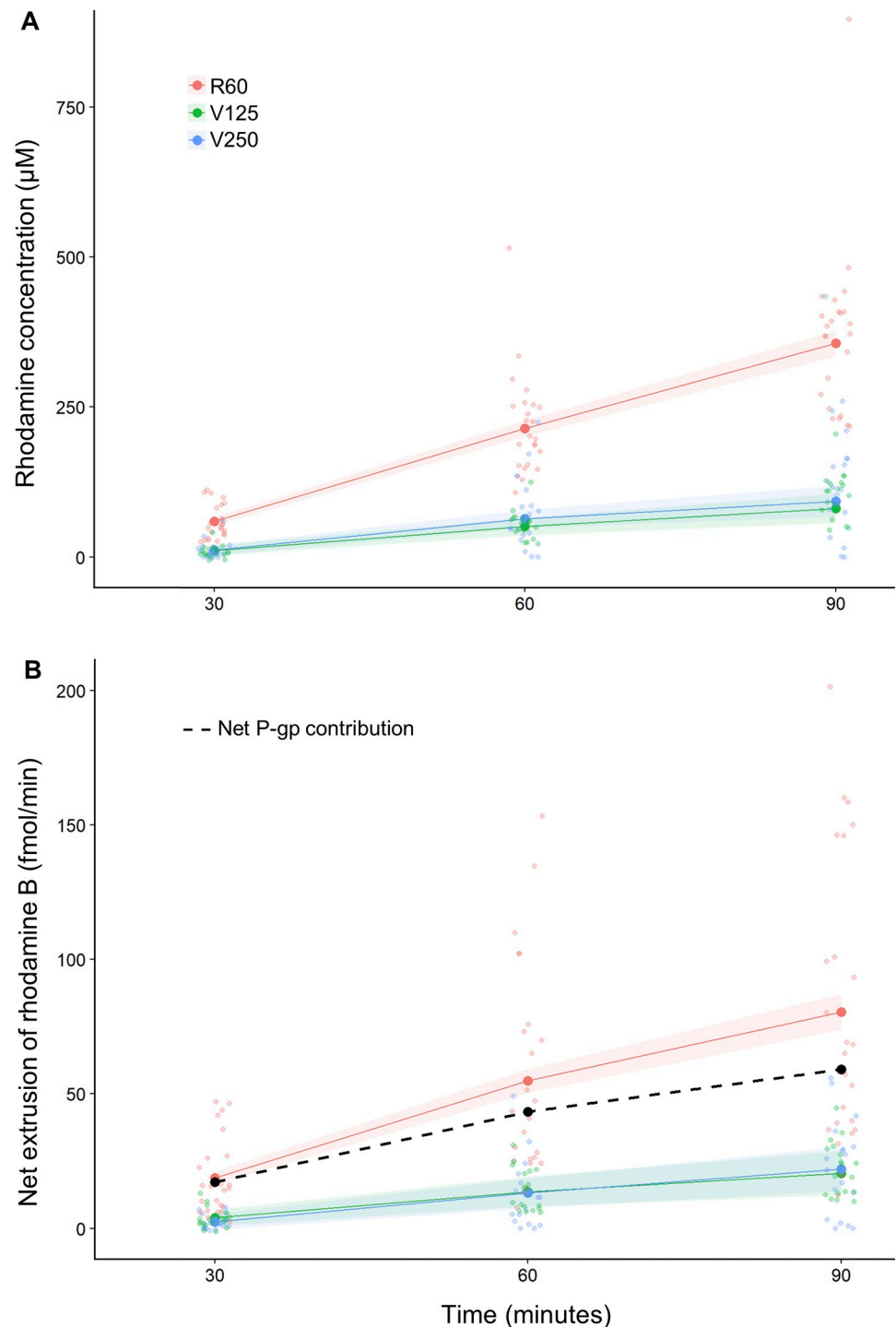


Fig 4. The mean rhodamine B concentration of the droplets secreted by the Malpighian tubules, and the mean net extrusion of rhodamine B increased over time in all the treatments. (A) The addition of verapamil (125 or 250 μM) reduced the rhodamine B concentration of the droplets secreted compared with the control treatment 60 μM rhodamine. (B) The addition of verapamil (125 μM or 250 μM) reduced the net extrusion of rhodamine B compared with the control treatment 60 μM rhodamine. The dashed line represents the net contribution of the P-glycoproteins obtained by subtracting the net extrusion of rhodamine in the V250 treatment from the R60. Each line with shaded region represents the mixed effect model fit with the standard error. Small circles represent the raw data.

<https://doi.org/10.1371/journal.pone.0223569.g004>

Table 2. The outcomes of linear mixed effect model used to investigate the effect of incubation time and treatment on the rhodamine concentration (μM) of the droplets secreted.

A.	Treatment	Time 30 min		Time 60 min		Time 90 min	
		Mean \pm se		Mean \pm se		Mean \pm se	
	R60	59.0 \pm 7.3		217.9 \pm 13.7		369.7 \pm 22.4	
	V125	9.0 \pm 8.5		54.0 \pm 15.8		103.4 \pm 25.9	
	V250	10.4 \pm 8.5		74.4 \pm 15.9		135.2 \pm 25.9	

B.	Treatment	Time 60 vs time 30 min		Time 90 vs time 60 min	
		estimate \pm se	P-value	estimate \pm se	P-value
	R60	158.9 \pm 11.8	< .001	151.8 \pm 11.8	< .001
	V125	45 \pm 13.6	0.004	49.4 \pm 13.6	0.001
	V250	64 \pm 13.7	< .001	60.8 \pm 13.7	< .001

C.	Treatment	Time 60 vs time 30 min		Time 90 vs time 60 min	
		estimate \pm se	P-value	estimate \pm se	P-value
	V125 vs R60	-113.9 \pm 18	< .001	-102.4 \pm 18	< .001
	V250 vs R60	-94.9 \pm 18.1	< .001	-91 \pm 18.1	< .001
	V250 vs V125	19 \pm 19.3	0.588	11.4 \pm 19.3	0.826

D.	Treatment	Time 30 min		Time 60 min		Time 90 min	
		estimate \pm se	P-value	estimate \pm se	P-value	estimate \pm se	P-value
	V125 vs R60	-49.98 \pm 11.2	< .001	-163.88 \pm 20.9	< .001	-266.31 \pm 34.2	< .001
	V250 vs R60	-48.59 \pm 11.2	< .001	-143.49 \pm 21.0	< .001	-234.53 \pm 34.2	< .001
	V250 vs V125	1.39 \pm 12.0	0.993	20.4 \pm 22.5	0.637	31.78 \pm 36.6	0.662

The model applied was (Rhodamine concentration \sim time * treatment + (1|locust) + (1+time|tubule)). (A) Summary of the mean values for each treatment at each time point. (B) Pairwise comparisons between time of incubation separately for each treatment. (C) Pairwise comparison of the interaction between time and treatment. D) Pairwise comparisons between treatments separately for each time of incubation.

<https://doi.org/10.1371/journal.pone.0223569.t002>

The surface area positively influenced the net extrusion of rhodamine B in the tubules incubated for 60 and 90 minutes in the R60 treatment, while there was no correlation between surface area and net extrusion in V125 and V250 treatments (Table 3E, Fig 5A–5C). In addition, we found that after 30 minutes the fluid secretion rate of the tubules incubated in R60 positively influenced the net extrusion of rhodamine B, while there was no significant effect in the V125 and V250 treatments (Table 3F, Fig 5D). After 60 and 90 minutes, the fluid secretion rate positively correlated with the net extrusion of rhodamine B in R60 and V250 treatments, but not V125 (Table 3F, Fig 5E and 5F). Moreover, the secretion rate of the tubules incubated in R60 showed a more pronounced effect on the net extrusion of rhodamine B than that of the tubules incubated in V125 and V250 (Table 3G, Fig 5D–5F).

Net contribution of P-glycoproteins

A single Malpighian tubule with a mean surface area incubated in a solution of 60 μM rhodamine B, extruded rhodamine B with a rate of 19.5 ± 2.6 fmol/min in the first 30 minutes, 58.9 ± 4.7 fmol/min between 30 and 60 minutes and 87.4 ± 7.0 fmol/min between 60 and 90 minutes (Table 3A). The addition of verapamil significantly reduced the quantity of rhodamine B extruded but did not block it completely (Table 3A). The rhodamine B concentration of the droplets secreted did not differ between the V125 and V250 treatments (Table 2A). Therefore, we assumed that 125 μM verapamil was sufficient to inhibit all the P-glycoproteins

Table 3. Outcomes of a linear mixed model to investigate the effect of incubation time and treatment on the net quantity of rhodamine extruded (fmol/min) in the droplets secreted per minute.

A.	Treatment	Time 30 min	Time 60 min	Time 90 min	Total		
		Mean \pm se	Mean \pm se	Mean \pm se	Mean		
	R60	19.5 \pm 2.5	58.9 \pm 4.7	87.4 \pm 7.0	165.8		
	V125	3.7 \pm 2.8	14.0 \pm 5.3	21.5 \pm 8.0	39.2		
	V250	2.3 \pm 2.9	13.5 \pm 5.4	22.2 \pm 8.0	38		
	Net P-gp contribution	17.2 (88%)	45.4 (77%)	65.2 (75%)	127.8 (77%)		

B.	Treatment	Time 60 vs time 30 min		Time 90 vs time 60 min			
		estimate \pm se	P-value	estimate \pm se	P-value		
	R60	39.5 \pm 3.1	< .001	28.5 \pm 3.1	< .001		
	V125	10.3 \pm 3.5	0.013	7.5 \pm 3.5	0.092		
	V250	11.2 \pm 3.6	0.006	8.7 \pm 3.6	0.046		

C.	Treatment	Time 60 vs time 30 min		Time 90 vs time 60 min			
		estimate \pm se	P-value	estimate \pm se	P-value		
	V125 vs R60	-29.2 \pm 4.7	< .001	-21.0 \pm 4.7	< .001		
	V250 vs R60	-28.2 \pm 4.8	< .001	-19.8 \pm 4.8	< .001		
	V250 vs V125	1.0 \pm 5.0	0.981	1.2 \pm 5.0	0.971		

D.	Treatment	Time 30 min		Time 60 min		Time 90 min	
		estimate \pm se	P-value	estimate \pm se	P-value	estimate \pm se	P-value
	V125 vs R60	-15.8 \pm 3.8	< .001	-44.9 \pm 7.1	< .001	-65.9 \pm 10.6	< .001
	V250 vs R60	-17.2 \pm 3.8	< .001	-45.4 \pm 7.1	< .001	-65.2 \pm 10.7	< .001
	V250 vs V125	-1.4 \pm 4	0.937	-0.4 \pm 7.6	0.998	0.7 \pm 11.3	0.998

E.	Treatment	Time 30 min		Time 60 min		Time 90 min	
		surf. trend \pm se	P-value	surf. trend \pm se	P-value	surf. trend \pm se	P-value
	R60	4.1 \pm 3.8	0.287	23.4 \pm 7.0	0.002	40.2 \pm 10.5	< .001
	V125	-1.1 \pm 4.8	0.818	2.2 \pm 8.9	0.803	5.2 \pm 13.3	0.698
	V250	-1.1 \pm 4.4	0.811	2.2 \pm 8.2	0.793	0.9 \pm 12.2	0.943

F.	Treatment	Time 30 min		Time 60 min		Time 90 min	
		SR trend \pm se	P-value	SR trend \pm se	P-value	SR trend \pm se	P-value
	R60	63.1 \pm 7.2	< .001	192.1 \pm 11.0	< .001	254.4 \pm 15.2	< .001
	V125	12.4 \pm 7.4	0.749	30.4 \pm 17.2	0.081	42.5 \pm 34.3	0.219
	V250	-4.1 \pm 5.2	0.429	53.4 \pm 12.1	< .001	79.2 \pm 22.5	< .001

G.	Treatment	Time 30 min		Time 60 min		Time 90 min	
		estimate \pm se	P-value	estimate \pm se	P-value	estimate \pm se	P-value
	R60 vs V125	60.7 \pm 10.3	< .001	161.7 \pm 20.45	< .001	211.9 \pm 37.5	< .001
	R60 vs V250	67.2 \pm 8.8	< .001	138.6 \pm 16.4	< .001	175.2 \pm 27.2	< .001
	V125 vs V250	6.5 \pm 9.0	0.754	-23.0 \pm 21.1	0.522	-36.7 \pm 41.1	0.645

The model applied was (Net extrusion of rhodamine \sim surface \times time \times treatment + (1|locust) + (1+time|tubule)). (A) Summary of the mean value for each treatment at each time point. (B) Pairwise comparisons between time of incubation separately for each treatment. (C) Pairwise comparison of the interaction between time and treatment. (D) Pairwise comparisons between treatments separately for each time of incubation. (E) Estimates of the influence of each unit of surface (mm²) on the quantity of rhodamine extruded at each time point. (F,G) Outcomes of the linear mixed effects model to investigate the effect of the secretion rate (SR) on the quantity of rhodamine extruded in the droplets secreted. The model applied was (Net extrusion of rhodamine \sim secretion rate \times treatment \times time + (1|locust) + (1+time|tubule)). The means estimate the influence of each nL/min of secretion rate on the quantity of rhodamine extruded.

<https://doi.org/10.1371/journal.pone.0223569.t003>

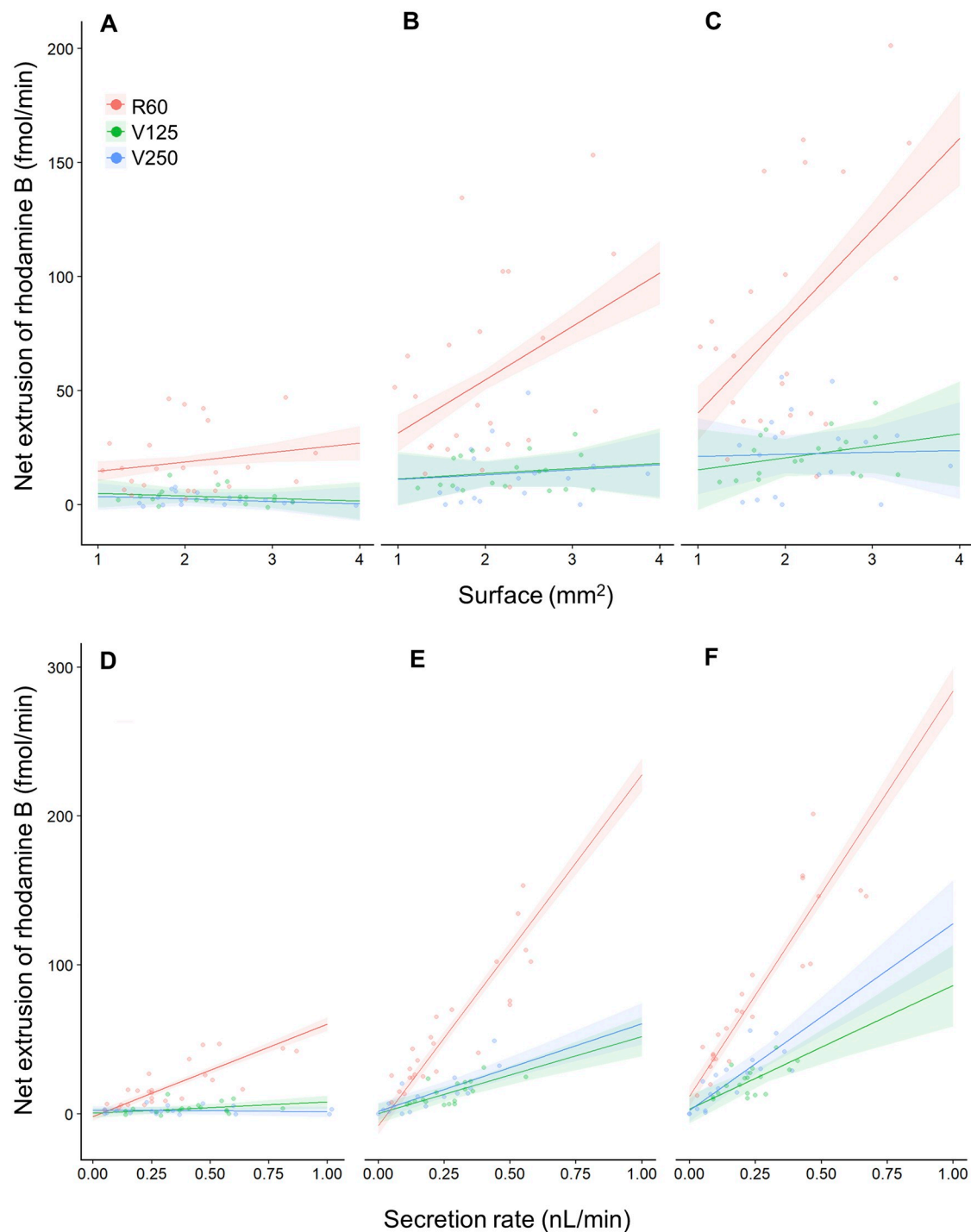


Fig 5. Tubule surface area and the fluid secretion rate positively influences the net extrusion of rhodamine B. (A) A plot of the surface area of the tubule exposed to the bath versus the net extrusion of rhodamine B for each of the three treatments after 30 minutes of incubation. (B) As in 'A' but after 60 minutes. (C) As in 'A' but after 90 minutes. (D) A plot of the fluid secretion rate versus the net extrusion of rhodamine B for each of the three treatments after 30 minutes of incubation. (E) As in 'D' but after 60 minutes. (F) As in 'D' but after 90 minutes. Small circles indicate the net extrusion of rhodamine B of individual tubules at a particular time point. Each line with the shaded area around represents the mixed effect model fit with the standard error.

<https://doi.org/10.1371/journal.pone.0223569.g005>

that are verapamil sensitive and that passive diffusion and other types of pumps may contribute to extrusion of Rhodamine B. We subtracted the mean values of the net extrusion of rhodamine B obtained from the V250 treatment from the net extrusion of the R60 treatment to estimate the contribution of the P-glycoproteins alone. The average rates of rhodamine B extruded by the P-glycoproteins were 17.2 fmol/min, 45.4 fmol/min and 65.2 fmol/min between 0–30, 30–60 and 60–90 minutes respectively (Table 3A, Fig 4B dashed line). In percentage, the P-glycoproteins are responsible for the 88%, 77% and 75% (between 0–30, 30–60 and 60–90 minutes respectively) of the total extrusion of rhodamine B. Overall, P-glycoproteins account for the 77% of the total extrusion of rhodamine B, over the 90 minutes of incubation.

Discussion

Our aim was to determine whether P-glycoprotein transporters are involved in the removal of xenobiotic substances by Malpighian tubules from the haemolymph of desert locusts and, if so, how they perform physiologically. To this end, we developed an alternative method to liquid chromatography–mass spectrometry [37], radiolabelled alkaloids [9] or confocal microscopy [11,12] based upon measuring dye concentration. A similar method has been used previously to investigate epithelial transport in tardigrades and desert locusts using chlorophenol red by imaging through the gut or tubules [38]. By imaging extruded drops from Malpighian tubules, we assessed the performance of epithelial transporters more accurately than by imaging the lumen of the tubules. We used the P-glycoprotein substrate rhodamine B [25] and the P-glycoprotein inhibitor verapamil [39] to assay P-glycoprotein function through the colour of the droplets secreted by the Malpighian tubules. Using this strategy, we obtained evidence that desert locust Malpighian tubules express a P-glycoprotein transporter, that the fluid secretion rate of these tubules is proportional to their surface area, and that the fluid secretion rate influences the net extrusion of rhodamine B.

A P-glycoprotein transporter extrudes xenobiotics in desert locust Malpighian tubules

Our conclusion that desert locust Malpighian tubules express P-glycoproteins is supported by two lines of evidence. Firstly, these tubules actively extrude the dye rhodamine B, a P-glycoprotein substrate (e.g. [25,26]), when it is present in the solution in which they are incubated. Rhodamine B has been widely used as a substrate for P-glycoproteins in cell culture and blood brain barrier models (e.g. [25,26]). Secondly, the addition of verapamil, a P-glycoprotein inhibitor (e.g. [23,27,28,39]), significantly reduced the extrusion of rhodamine B. The presence of P-glycoproteins in other tissues of the desert locusts also supports our conclusion that they are expressed in the Malpighian tubules; proteins with a comparable physiology and similar sequence to the human P-glycoprotein (ABCB1 gene) are expressed within the blood brain barrier of the locusts *S. gregaria* and *L. migratoria* [23,37,40,41]. Further support comes from comparison with other insects; P-glycoprotein transporters have been found in the Malpighian tubules of many other insects including the black field cricket (*Teleogryllus commodus* [11]), tobacco hornworm (*Manduca sexta* [9,42]), fruit fly (*D. melanogaster*), kissing bug (*Rhodnius prolixus*), large milkweed bug (*Oncopeltus fasciatus*), yellow fever mosquito (*Aedes aegypti*), house cricket (*Acheta domestica*), migratory locust (*Locusta migratoria*), mealworm beetle (*Tenebrio molitor*), and the American cockroach (*Periplaneta americana*) [15].

Rhodamine B extrusion was not blocked entirely by 125 μ M verapamil or by double this concentration. Comparison of the extent of the reduction at both concentrations suggests that even at the lower verapamil concentration all the P-glycoproteins were inhibited. This suggests

that approximately 77% of rhodamine B was transported by P-glycoproteins via a verapamil sensitive mechanism, whilst the remaining 23% was verapamil insensitive. Moreover, after 90 minutes the concentration of rhodamine B in the droplets secreted by the Malpighian tubules was higher than that of the bathing solution suggesting that rhodamine B transport in the presence of verapamil is not simply due to passive diffusion, but that other active transporters may be implicated. Several potential candidates for alternative active transporters exist. For example, in human cell lines (Calu-3), rhodamine B can interact with multiple organic cation transporters (OCT3, OCTN1,2) [43]. Potentially, however, verapamil may be incapable of blocking rhodamine B transport completely allowing a small number of rhodamine B molecules to be extruded by the P-glycoprotein even in the presence of verapamil.

Verapamil inhibits P-glycoproteins and does not interact with other multidrug resistance proteins [44]. This suggests that the effects of verapamil in our experiments are through its specific effects upon P-glycoproteins. The mechanistic basis of verapamil inhibition is unclear but the most widely accepted explanation is that P-glycoproteins extrude both verapamil and their substrate but that verapamil diffuses back across the lipid bilayer much faster than the substrate creating a futile cycle and thereby competing with the substrate transport [45,46].

Verapamil is, however, also a known L-type Ca^{2+} channel blocker [47]. In *Drosophila*, L-type Ca^{2+} channels are expressed in the basolateral and apical membranes of the tubule principal cells, and are involved in the regulation of the fluid secretion [48]. Indeed, an increase of the intracellular Ca^{2+} level mediates the effect of diuretic hormones [49]. Verapamil reduced the fluid secretion of *Drosophila* Malpighian tubules stimulated by peptide agonists (e.g. CAP2b, cGMP) but had no effect on unstimulated tubules [48]. Our experiments cannot exclude the possibility that verapamil affects Ca^{2+} channels in locust Malpighian tubules by interfering with intracellular Ca^{2+} , and thereby has an indirect effect on Rhodamine B extrusion. However, because the fluid secretion rate did not differ between treatments, the reduction in the net extrusion of rhodamine B was likely caused solely by verapamil inhibition of the P-glycoproteins. Thus, when considered within the context of the expression of P-glycoproteins in the blood brain barrier of locusts [23,37,40,41] and the expression of P-glycoproteins in homologous Malpighian tubules in other insects species (see above), it seems highly likely that the tubules of gregarious desert locust express P-glycoproteins.

Malpighian tubule surface area and fluid secretion rate

We used linear mixed effect models to determine which physical feature of a tubule, its surface area, length or diameter has the greatest influence on fluid secretion rate. We found that the surface area of the Malpighian tubules positively influences their fluid secretion rate, and more accurately predicts the fluid secretion rate than tubule diameter or length. Some previous studies have reported that tubule length was linearly related to the fluid secretion rate [50,51] but in our analysis length was consistently worse than surface area as a predictor. Even when the surface area (or length) has been accounted for in previous studies, this has involved dividing the fluid secretion rate by the surface area (or length) to obtain the fluid secretion rate per unit area (or unit length) [15,52]. Although this approach is useful when comparing tubules of different sizes from different insect species, it fails to reveal the exact relationship between the surface area and the fluid secretion rate. Our statistical models demonstrate that interactions between factors such as surface area and fluid secretion rate depend upon the treatment applied. For example, our results show that the fluid secretion rate increases with the increasing of the tubule surface in all the treatments apart from 250 μM verapamil, where the surface no longer influences the fluid secretion rate. Such interdependencies are unlikely to be

detected or accounted for in simpler statistical analyses, causing such interdependencies to be ignored.

Reliability of isolated Malpighian tubule measurements

The decrease in fluid secretion rate that we found is comparable with other studies of isolated Malpighian tubules, where the fluid secretion rate of tubules incubated in saline decreased of 30% after 20 minutes [53] or over one hour [54]. In contrast, fluid secretion rates have been found steady over time in studies where the Malpighian tubules were left attached to the gut through the tracheae, and the whole preparation immersed in saline [6,55]. One of the differences between the isolated tubule assay and the whole gut assay is the shorter portion of trachea in contact with the tubule immersed in the bathing solution. Therefore, the reduction of the fluid secretion rate in isolated tubules may be a consequence of a smaller amount of residual oxygen in the tracheae compared with the whole gut preparation. Additionally, the volume of the bathing solution in the isolated tubule assay is far smaller than in the whole gut preparation, which could lead to a quicker depletion of oxygen and/or other substances in the bathing solution. Replacing the bathing solution with fresh saline produced an increase in the fluid secretion rate, supporting this interpretation. Finally, there could be a decrease in the tubule diameter during the assay compared to the *in vivo* preparation. We can safely exclude this, however, because we found that the tubule diameter was unaffected by the assay and was similar to the tubule's diameter *in vivo*.

Determining the transepithelial transport of xenobiotics by P-glycoprotein transporters in locust Malpighian tubules

Transepithelial transport of xenobiotics by P-glycoproteins across the inner membrane of the Malpighian tubules can be determined from the net extrusion rate we measured. The disparity between the transepithelial transport and the net extrusion rate is due to the properties of rhodamine B. This lipophilic dye can passively permeate the lipid bilayer of liposomes, following the concentration gradient [25]. Likewise, in desert locust Malpighian tubules, rhodamine B can back diffuse into the bath solution when active transporters increase its luminal concentration creating a concentration gradient. Consequently, the fluid secretion rate affects the net extrusion rate of rhodamine B because a decrease in the fluid secretion will increase the luminal concentration of the dye, allowing greater back diffusion whilst an increase in the fluid secretion rate will have the opposite effect [1]. Therefore, if a dye, like rhodamine B, can back diffuse, its net extrusion will be proportional to the fluid secretion rate (S6A–S6C Fig), while if the dye cannot back diffuse there will be no correlation (S6D–S6F Fig). When the rhodamine B concentration in the lumen was lower or similar to the bath (60 μ M) the net transport would be little affected by the secretion rate. Conversely, when the luminal rhodamine B concentration was higher than the bathing solution, part of the dye diffused back, so that the net extrusion was significantly influenced by the fluid secretion rate.

Previous studies demonstrated that Malpighian tubules can exhibit different degrees of passive permeability to different substances, depending on the species and on the properties (i.e. size, polarity) of the substrate used (e.g. dyes, alkaloid, drugs) [1]. For example, tubules of the kissing bug (*R. prolixus*) have passive permeability to the alkaloid nicotine [8], but not to the dye indigo carmine [1], whereas tubules of the blowfly (*Calliphora erythrocephala*) are permeable to indigo carmine [1]. Thus, when studying the effect of a substance on active transporters, it is important to take into account the fluid secretion rate because a change in the net extrusion rate of a substrate may be caused not only by a direct effect on the transporters, but also by an indirect consequence of a change in the fluid flow [12]. In our experiment, the fluid

secretion rate did not differ between treatments, indicating that the reduction of net extrusion of rhodamine B following exposure to verapamil was caused solely by inhibition of the P-glycoprotein. However, the fluid secretion rate decreased over time, which may produce an underestimation of the net transepithelial transport of rhodamine B.

Implications for desert locust xenobiotic extrusion

Gregarious desert locusts feed on a broad variety of plants including species containing secondary metabolites such as atropine to become unpalatable to predators [17–20]. The expression of P-glycoproteins in the Malpighian tubules to extrude noxious substances may be an adaptation to cope with the ingestion of toxic plants. This may also be the reason for expression of P-glycoproteins on the blood brain barrier of desert locusts, which would prevent the uptake of hydrophobic substances in the central nervous system [23]. Yet the relationship between ingesting toxins and xenobiotic extrusion pathways in the Malpighian tubules is not straightforward; some species of Orthoptera, as well as Coleoptera, Lepidoptera, Heteroptera, Hymenoptera and Sternorrhyncha [56], sequester toxins from the plants they ingest to deter predators. However, toxicity may also be conferred by gut contents, rather than through sequestration within bodily tissues. For example, the chemical defence of the spotted bird grasshopper, *Schistocerca emarginata* (= *lineata*), is mediated by the contents of toxic plant in its gut [21,22]. This species is a congener of the desert locust, *S. gregaria*, which suggests that a similar strategy may be involved in the production of toxicity in this species. If this is the case, then the presence of toxins in the haemolymph may be a consequence of ingesting toxic plant material for storage within the gut. In such a scenario, xenobiotic extrusion pathways within the Malpighian tubules would then be essential for ensuring that toxins do not accumulate within the haemolymph to concentrations that would affect physiological processes.

The P-glycoprotein xenobiotic extrusion pathway that we have characterised in desert locusts is likely to be highly effective in extruding xenobiotic compounds from haemolymph, especially when the number of Malpighian tubules within an individual locust is considered. However, it is important to consider that the locusts used for our experiments have experienced a diet free of toxins, such as atropine. P-glycoprotein expression can be modulated depending on the diet [57]; *Drosophila* larvae fed on colchicine increased the expression of the P-glycoprotein gene homologue *mdr49* in the brain and gut. Consequently, adult gregarious desert locusts that have fed on a diet including plant toxins may have even stronger P-glycoprotein xenobiotic extrusion pathways. In contrast to their gregarious counterparts, solitary desert locusts actively avoid plants containing atropine [17], and find odours associated with it aversive [58]. Thus, Malpighian tubules of solitary desert locusts may express fewer P-glycoproteins than those of the gregarious phase, possibly due to their reduced exposure to secondary metabolites from their diet.

Implications for insect pest control

P-glycoproteins are implicated in the resistance of some insect pests to insecticides [59] promoting the efflux of various xenobiotics thereby decreasing the intracellular drug accumulation. For instance, P-glycoproteins have been detected in a resistant strain of the pest cotton bollworm (*Helicoverpa armigera*) but not in a susceptible one [60]. P-glycoproteins have also been implicated in the protection of the mitochondria from insecticide damage [61]. In Africa and Asia, applications of insecticides are carried out to try to control desert locust plagues [62]. To increase the efficacy, a combination of P-glycoprotein inhibitors and insecticide may act synergistically to increase the locust mortality, reducing the amount of insecticide used.

Further investigation into the interaction between P-glycoproteins and different xenobiotics (i.e. insecticides, herbicides, miticides and secondary metabolites) may improve our understanding of the physiological effect of pesticides on insects, and subsequently lead to the development of more specific targeted insecticides.

Supporting information

S1 Fig. Examples of the droplets secreted by the Malpighian tubules of desert locusts during the incubation in each of the different treatments every 30 minutes. The size of each droplet depends upon the fluid secretion rate whilst the colour is determined by the net extrusion rate of rhodamine B.

(TIF)

S2 Fig. Calibration lines used to determine the rhodamine B concentration in the droplets secreted by the Malpighian tubules. For each droplet diameter rank there is a linear relationship between the rhodamine concentration of the droplet and the colour intensity measured. The slope of the lines decreases as the diameter increases. We estimated the rhodamine B concentration of the droplets secreted by measuring the colour intensity and the diameter of each droplet. Each line represents the linear regression fit for each mean diameter rank.

(TIF)

S3 Fig. The relationship between intensity and rhodamine B concentration depends upon droplet diameter. (A) The slope decreases as the diameter increases, following an exponential decay. (B) After log transformation the relationship becomes linear. Using this linear equation for each droplet diameter measured, we predicted the slope of the line equation that link the colour intensity to the rhodamine concentration.

(TIF)

S4 Fig. Mean fluid secretion rate of Malpighian tubules increases with fresh saline. The tubules were incubated in saline but after 90 minutes the saline bath was removed and replaced with fresh saline. The arrow indicates the first measurement taken after the saline had been replaced. Grey points indicate the fluid secretion rate of individual tubules at a particular time point.

(TIF)

S5 Fig. Manipulation of Malpighian tubules in the Ramsay assay did not affect their diameter. To exclude the possibility that manipulation during the assay affected tubule morphology, we measured the tubule's diameter *in vivo*, at the beginning, and at the end of the assay. The diameter was unaffected by the manipulation.

(TIF)

S6 Fig. Schematic representation of the influence of the back diffusion on the net extrusion of a dye. (A) The net extrusion of a dye positively correlates with the fluid secretion rate when the dye can back diffuse from the lumen to the bathing fluid. (B) Indeed, at low fluid secretion rate, the dye concentration in the lumen rises, increasing the back diffusion and reducing the net transport of the dye. (C) Instead, at higher fluid secretion rates, the dye concentration in the lumen is diluted and the back diffusion is reduced, increasing the net transport of the dye. (D) If no back diffusion occurs, there is no correlation between the net transport of the dye and the fluid secretion rate. (E,F) At any rate of fluid secretion, the net transport of the dye remains constant, independently of the dye concentration in the lumen.

(TIF)

S1 Table. Comparison of linear mixed effect models incorporating length, diameter or surface area. Based on the lowest AIC parameter, the surface area was the best explanatory variable for the secretion rate. The row in bold indicates the model with the lowest AIC. Only the fixed effects are shown.

(TIF)

S2 Table. Outcomes of the linear mixed effect model investigating the effect the replacement of the saline with a fresh saline after 90 minutes of incubation upon the fluid secretion rate. The model applied was (Secretion rate ~ surface + time + (1|locust) + (1+time|tubule)). The rows in bold indicate the first observation after the saline has been replaced.

(A) Summary of the mean values of fluid secretion rate at each time point. (B) Pairwise comparisons between subsequent times of incubation.

(TIF)

S3 Table. Outcomes of the linear mixed effect model investigating the diameter of the tubules in different moments during the Ramsay assay. The model applied was (diameter ~ assay time + (1|locust) + (1+time|tubule)). (A) Summary of the mean diameter of Malpighian tubules *in vivo*, at the beginning of the assay and at the end of the assay after 180 minutes of incubation. (B) Pairwise comparisons between different moments of the assay.

(TIF)

S1 File. Raw data. Total number of observations used for the analysis of the rhodamine and verapamil experiment.

(XLSX)

S2 File. Raw data. Total number of observations used for the analysis of the renewing of the bath saline experiment.

(XLSX)

S3 File. Raw data. Total number of observations used for the analysis of the comparison of the tubule diameter *in vivo*, at the beginning and at the end of the assay.

(XLSX)

Acknowledgments

M.R. was financially supported by a graduate studentship from the School of Life Sciences, University of Sussex. D.D.B was financially supported by the Welsh government/HEFCW RESILCOAST project.

Author Contributions

Data curation: Marta Rossi.

Formal analysis: Marta Rossi, Davide De Battisti.

Funding acquisition: Jeremy Edward Niven.

Investigation: Marta Rossi.

Methodology: Marta Rossi, Jeremy Edward Niven.

Project administration: Jeremy Edward Niven.

Supervision: Jeremy Edward Niven.

Visualization: Marta Rossi.

Writing – original draft: Marta Rossi.

Writing – review & editing: Marta Rossi, Jeremy Edward Niven.

References

1. Maddrell SH, Gardiner BO, Pilcher DE, Reynolds SE. Active transport by insect Malpighian tubules of acidic dyes and of acylamides. *J Exp Biol.* 1974 Oct 1; 61(2):357–77. PMID: [4443733](#)
2. Ramsay JA. Excretion by the Malpighian tubules of the stick insect, *Dixippus morosus* (Orthoptera, Phasmidae): amino acids, sugars and urea. *J Exp Biol.* 1958 Dec 1; 35(4):871–91.
3. Phillips JE. Rectal absorption in the desert locust, *Schistocerca gregaria* Forskal. I. *J Exp Biol.* 1964 Mar; 41:15–38. PMID: [14161606](#)
4. O'Donnell M. Insect excretory mechanisms. *Adv In Insect Phys.* 2008 Jan 1; 35:1–122.
5. Williams JC, Hagedorn HH, Beyenbach KW. Dynamic changes in flow rate and composition of urine during the post-bloodmeal diuresis in *Aedes aegypti* (L.). *J Comp Physiol B.* 1983 Jun 21; 153(2):257–65.
6. Maddrell SH, Klunswan S. Fluid secretion by in vitro preparations of the Malpighian tubules of the desert locust *Schistocerca gregaria*. *J Insect Physiol.* 1973 Jul 1; 19(7):1369–76.
7. Wieczorek HE. The insect V-ATPase, a plasma membrane proton pump energizing secondary active transport: molecular analysis of electrogenic potassium transport in the tobacco hornworm midgut. *J Exp Biol.* 1992 Nov 1; 172(1):335–43.
8. Maddrell SH, Gardiner BO. Excretion of alkaloids by Malpighian tubules of insects. *J Exp Biol.* 1976 Apr 1; 64(2):267–81. PMID: [932618](#)
9. Gaertner LS, Murray CL, Morris CE. Transepithelial transport of nicotine and vinblastine in isolated Malpighian tubules of the tobacco hornworm (*Manduca sexta*) suggests a P-glycoprotein-like mechanism. *J Exp Biol.* 1998 Sep 15; 201(18):2637–45.
10. Karnaky KJ Jr, Petzel D, Sedmerova M, Gross A, Miller DS. Mrp2-like transport of Texas Red by Malpighian tubules of the common American cockroach, *Periplaneta americana*. *Bull Mt Des Isl Biol Lab.* 2000; 39:52–3.
11. Leader JP, O'Donnell MJ. Transepithelial transport of fluorescent p-glycoprotein and MRP2 substrates by insect Malpighian tubules: confocal microscopic analysis of secreted fluid droplets. *J Exp Biol.* 2005 Dec 1; 208(23):4363–76.
12. O'Donnell MJ, Leader JP. Changes in fluid secretion rate alter net transepithelial transport of MRP2 and P-glycoprotein substrates in Malpighian tubules of *Drosophila melanogaster*. *Arch Insect Biochem Physiol: Published in Collaboration with the Entomological Society of America.* 2006 Nov; 63(3):123–34.
13. Wright SH, Dantzer WH. Molecular and cellular physiology of renal organic cation and anion transport. *Physiol Rev.* 2004 Jul; 84(3):987–1049. <https://doi.org/10.1152/physrev.00040.2003> PMID: [15269342](#)
14. Hawthorne DJ, Dively GP. Killing them with kindness? In-hive medications may inhibit xenobiotic efflux transporters and endanger honey bees. *PLoS One.* 2011 Nov 2; 6(11):e26796. <https://doi.org/10.1371/journal.pone.0026796> PMID: [22073195](#)
15. Rheault MR, Plaumann JS, O'Donnell MJ. Tetraethylammonium and nicotine transport by the Malpighian tubules of insects. *J Insect Physiol.* 2006 May 1; 52(5):487–98. <https://doi.org/10.1016/j.jinsphys.2006.01.008> PMID: [16527303](#)
16. Guseman AJ, Miller K, Kunkle G, Dively GP, Pettis JS, Evans JD, Hawthorne DJ. Multi-drug resistance transporters and a mechanism-based strategy for assessing risks of pesticide combinations to honey bees. *PLoS One.* 2016 Feb 3; 11(2):e0148242. <https://doi.org/10.1371/journal.pone.0148242> PMID: [26840460](#)
17. Despland E, Simpson SJ. Food choices of solitary and gregarious locusts reflect cryptic and aposematic antipredator strategies. *Anim Behav.* 2005 Feb 1; 69(2):471–9.
18. Mainguet AM, Louveaux A, El Sayed G, Rollin P. Ability of a generalist insect, *Schistocerca gregaria*, to overcome thioglucoside defense in desert plants: tolerance or adaptation?. *Entomol Exp Appl.* 2000 Mar; 94(3):309–17.
19. Sword GA, Simpson SJ, El Hadi OT, Wilps H. Density-dependent aposematism in the desert locust. *Proc R Soc Lond B Biol Sci.* 2000 Jan 7; 267(1438):63–8.
20. Pener MP, Simpson SJ. Locust phase polyphenism: an update. *Adv Insect Phys.* 2009 Jan 1; 36:1–272.

21. Sword GA. Tasty on the outside, but toxic in the middle: grasshopper regurgitation and host plant-mediated toxicity to a vertebrate predator. *Oecologia*. 2001 Aug 1; 128(3):416–21. <https://doi.org/10.1007/s004420100666> PMID: 24549911
22. Sword GA. Density-dependent warning coloration. *Nature*. 1999 Jan; 397(6716):217.
23. Andersson O, Badisco L, Hansen AH, Hansen SH, Hellman K, Nielsen PA, et al. Characterization of a novel brain barrier ex vivo insect-based P-glycoprotein screening model. *Pharmacol Res Perspect*. 2014 Aug; 2(4):e00050. <https://doi.org/10.1002/prp2.50> PMID: 25505597
24. Ramsay JA. Active transport of water by the Malpighian tubules of the stick insect, *Dixippus morosus* (Orthoptera, Phasmidae). *J Exp Biol*. 1954 Mar 1; 31(1):104–13.
25. Eytan GD, Regev R, Oren G, Hurwitz CD, Assaraf YG. Efficiency of P-glycoprotein-mediated exclusion of rhodamine dyes from multidrug-resistant cells is determined by their passive transmembrane movement rate. *Eur J Biochem*. 1997 Aug; 248(1):104–12. <https://doi.org/10.1111/j.1432-1033.1997.00104.x> PMID: 9310367
26. Mayer F, Mayer N, Chinn L, Pinsonneault RL, Kroetz D, Bainton RJ. Evolutionary conservation of vertebrate blood–brain barrier chemoprotective mechanisms in *Drosophila*. *J Neurosci*. 2009 Mar 18; 29(11):3538–50. <https://doi.org/10.1523/JNEUROSCI.5564-08.2009> PMID: 19295159
27. Dermauw W, Van Leeuwen T. The ABC gene family in arthropods: comparative genomics and role in insecticide transport and resistance. *Insect Biochem Mol Biol*. 2014 Feb 1; 45:89–110.
28. Hamada H, Hagiwara KI, Nakajima T, Tsuruo T. Phosphorylation of the Mr 170,000 to 180,000 glycoprotein specific to multidrug-resistant tumor cells: effects of verapamil, trifluoperazine, and phorbol esters. *Cancer Res*. 1987 Jun 1; 47(11):2860–5. PMID: 3567906
29. Schneider CA, Rasband WS, Eliceiri KW. NIH Image to ImageJ: 25 years of image analysis. *Nature Methods*. 2012 Jun 28; 9(7):671. <https://doi.org/10.1038/nmeth.2089> PMID: 22930834
30. R Core Team. R: A language and environment for statistical computing. R J, 2012.
31. Bates D, Mächler M, Bolker B, Walker S. Fitting linear mixed-effects models using lme4. 2014 Jun 23. <https://arxiv.org/abs/1406.5823>
32. Akaike H. Information theory and an extension of the maximum likelihood principle. *Selected papers of Hirotugu Akaike*: Springer; 1998. p. 199–213
33. Kuznetsova A, Brockhoff PB, Christensen RH. lmerTest package: tests in linear mixed effects models. *J Stat Softw*. 2017; 82(13).
34. Forstmeier W, Schielzeth H. Cryptic multiple hypotheses testing in linear models: overestimated effect sizes and the winner's curse. *Behav Ecol Sociobiol*. 2011 Jan 1; 65(1):47–55. <https://doi.org/10.1007/s00265-010-1038-5> PMID: 21297852
35. Lenth R, Lenth MR. Package 'lsmeans'. *Am Stat*. 2018 Nov 2; 34(4):216–21.
36. Wickham H. ggplot2: elegant graphics for data analysis. Springer; 2016 Jun 8.
37. Andersson O, Hansen SH, Hellman K, Olsen LR, Andersson G, Badolo L, et al. The grasshopper: a novel model for assessing vertebrate brain uptake. *J Pharmacol Exp Ther*. 2013 Aug 1; 346(2):211–8. <https://doi.org/10.1124/jpet.113.205476> PMID: 23671124
38. Halberg KA, Møbjerg N. First evidence of epithelial transport in tardigrades: a comparative investigation of organic anion transport. *J Exp Biol*. 2012 Feb 1; 215(3):497–507.
39. Tsuruo T, Iida H, Tsukagoshi S, Sakurai Y. Overcoming of vincristine resistance in P388 leukemia *in vivo* and *in vitro* through enhanced cytotoxicity of vincristine and vinblastine by verapamil. *Cancer Res*. 1981 May 1; 41(5):1967–72. PMID: 7214365
40. Al-Qadi S, Schiøtt M, Hansen SH, Nielsen PA, Badolo L. An invertebrate model for CNS drug discovery: Transcriptomic and functional analysis of a mammalian P-glycoprotein ortholog. *Biochim Biophys Acta Gen Subj*. 2015 Dec 1; 1850(12):2439–51.
41. Nielsen PA, Andersson O, Hansen SH, Simonsen KB, Andersson G. Models for predicting blood–brain barrier permeation. *Drug Discov Today*. 2011 Jun 1; 16(11–12):472–5. <https://doi.org/10.1016/j.drudis.2011.04.004> PMID: 21513815
42. Murray CL, Quaglia M, Arnason JT, Morris CE. A putative nicotine pump at the metabolic blood–brain barrier of the tobacco hornworm. *J Neurobiol*. 1994 Jan; 25(1):23–34.
43. Ugwu MC, Oli A, Esimone CO, Agu RU. Organic cation rhodamines for screening organic cation transporters in early stages of drug development. *J Pharmacol Toxicol Methods*. 2016 Nov 1; 82:9–19. <https://doi.org/10.1016/j.vascn.2016.05.014> PMID: 27235784
44. Cole SP, Downes HF, Slovak ML. Effect of calcium antagonists on the chemosensitivity of two multidrug-resistant human tumour cell lines which do not overexpress P-glycoprotein. *Br J Cancer*. 1989 Jan; 59(1):42. <https://doi.org/10.1038/bjc.1989.9> PMID: 2569325

45. Eytan GD, Regev R, Oren G, Assaraf YG. The role of passive transbilayer drug movement in multidrug resistance and its modulation. *J Biol Chem*. 1996 May 31; 271(22):12897–902. <https://doi.org/10.1074/jbc.271.22.12897> PMID: 8662680
46. Sharom FJ. The P-glycoprotein efflux pump: how does it transport drugs?. *J Membr Biol*. 1997 Dec 24; 160(3):161–75. <https://doi.org/10.1007/s002329900305> PMID: 9425600
47. Abernethy DR, Schwartz JB. Calcium-antagonist drugs. *N Engl J Med*. 1999 Nov 4; 341(19):1447–57. <https://doi.org/10.1056/NEJM199911043411907> PMID: 10547409
48. MacPherson MR, Pollock VP, Broderick KE, Kean LA, O Connell FC, Dow JA, et al. Model organisms: new insights into ion channel and transporter function L-type calcium channels regulate epithelial fluid transport in *Drosophila melanogaster*. *Am J Physiol*. 2001 Feb 1; 280(1):C394–407.
49. Paluzzi JP, Yeung C, O'Donnell MJ. Investigations of the signaling cascade involved in diuretic hormone stimulation of Malpighian tubule fluid secretion in *Rhodnius prolixus*. *J Insect Physiol*. 2013 Dec 1; 59(12):1179–85. <https://doi.org/10.1016/j.jinsphys.2013.09.005> PMID: 24080126
50. Beyenbach KW, Oviedo A, Aneshansley DJ. Malpighian tubules of *Aedes aegypti*: five tubules, one function. *J Insect Physiol*. 1993 Aug 1; 39(8):639–48.
51. Coast GM. Fluid secretion by single isolated Malpighian tubules of the house cricket, *Acheta domesticus*, and their response to diuretic hormone. *Physiol Entomol*. 1988 Dec; 13(4):381–91.
52. Bradley TJ. Functional design of microvilli in the Malpighian tubules of the insect *Rhodnius prolixus*. *J Cell Sci*. 1983 Mar 1; 60(1):117–35.
53. Coast GM, Rayne RC, Hayes TK, Mallet AI, Thompson KS, Bacon JP. A comparison of the effects of two putative diuretic hormones from *Locusta migratoria* on isolated locust Malpighian tubules. *J Exp Biol*. 1993 Feb 1; 175(1):1–4.
54. Proux JP, Picquot M, Herault JP, Fournier B. Diuretic activity of a newly identified neuropeptide—the arginine-vasopressin-like insect diuretic hormone: use of an improved bioassay. *J Insect Physiol*. 1988 Jan 1; 34(10):919–27.
55. James PJ, Kershaw MJ, Reynolds SE, Charnley AK. Inhibition of desert locust (*Schistocerca gregaria*) Malpighian tubule fluid secretion by destruxins, cyclic peptide toxins from the insect pathogenic fungus *Metarhizium anisopliae*. *J Insect Physiol*. 1993 Sep 1; 39(9):797–804.
56. Opitz SE, Müller C. Plant chemistry and insect sequestration. *Chemoecology*. 2009 Sep 1; 19(3):117.
57. Tapadia MG, Lakhota SC. Expression of mdr49 and mdr65 multidrug resistance genes in larval tissues of *Drosophila melanogaster* under normal and stress conditions. *Cell stress Chaperones*. 2005 Mar; 10(1):7. PMID: 15832942
58. Simões PM, Niven JE, Ott SR. Phenotypic transformation affects associative learning in the desert locust. *Curr Biol*. 2013 Dec 2; 23(23):2407–12. <https://doi.org/10.1016/j.cub.2013.10.016> PMID: 24268415
59. Lanning CL, Fine RL, Corcoran JJ, Ayad HM, Rose RL, Abou-Donia MB. Tobacco budworm P-glycoprotein: biochemical characterization and its involvement in pesticide resistance. *Biochim Biophys Acta Gen Subj*. 1996 Oct 24; 1291(2):155–62.
60. Srinivas R, Udikeri SS, Jayalakshmi SK, Sreeramulu K. Identification of factors responsible for insecticide resistance in *Helicoverpa armigera*. *Comp Biochem Physiol C Toxicol Pharmacol*. 2004 Mar 1; 137(3):261–9. <https://doi.org/10.1016/j.cca.2004.02.002> PMID: 15171950
61. Akbar SM, Aurade RM, Sharma HC, Sreeramulu K. Mitochondrial P-glycoprotein ATPase contributes to insecticide resistance in the cotton bollworm, *Helicoverpa armigera* (Noctuidae: Lepidoptera). *Cell Biochem Biophys*. 2014 Sep 1; 70(1):651–60. <https://doi.org/10.1007/s12013-014-9969-5> PMID: 24756730
62. Van Huis A. Strategies to control the Desert Locust *Schistocerca gregaria*. In: Vreysen MJB, Robinson AS, and Hendrichs J, editors. Area-wide control of insect pests. From research to field implementation. Springer, Dordrecht; 2007. p. 285–296.